Modulation of Electronic Coupling across Dioxolene-Bridged Osmium and Ruthenium Dinuclear Complexes

ARTICLE *in* INORGANIC CHEMISTRY · OCTOBER 1998

Impact Factor: 4.76 · DOI: 10.1021/ic980293l

Modulation of Electronic Coupling across Dioxolene-Bridged Osmium and Ruthenium Dinuclear Complexes

Tia E. Keyes,[†] Robert J. Forster,[†] Pradeep M. Jayaweera,[‡] Colin G. Coates,[‡] John J. McGarvey,[‡] and Johannes G. Vos*,[†]

Inorganic Chemistry Research Center, School of Chemical Sciences, Dublin City University, Dublin 9, Ireland, and School of Chemistry, The Queens University of Belfast, Belfast BT9 5AG, N. Ireland

Received March 16, 1998

The extent of metal−ligand orbital mixing and the degree of electronic coupling between $[M(bpy)_2]^{2+}$ fragments linked through a redox active 1,4-dihydroxy-2,5-bis(pyrazol-1′-yl)benzene (p-L) bridge is described, where M is Os or Ru and bpy is 2,2′-bipyridyl. This is the first reported example of osmium and ruthenium/osmium metals linked across a 1,4-dioxolene bridge. In fast scan cyclic voltammetry, the redox processes are reversible and four distinct one-electron processes are observed for the bridge and metal centers in the homo- and heterodinuclear complexes. The potential at which the first oxidation step occurs does not depend on the identity of the metal center. UV/vis spectroelectrochemistry, together with resonance Raman spectroscopy, suggests that the first two oxidation steps occur on the bridging ligand. For all complexes, an orbital mixing gradient occurs; metal−ligand orbital mixing increases in the order HQ ≪ SQ < Q (HQ is the reduced hydroquinone bridge, SQ the semiquinone, and Q the quinone), and M−L orbital mixing is enhanced in ruthenium compared with osmium. Analysis of the bipyridyl reductions shows that metal−metal coupling across the HQ bridge is essentially absent. For the first time, stable M(III) polypyridyl quinone complexes are reported. Electrochemical data suggest that communication across the quinone bridge is extensive, with substantial stabilization of the metal$^{II/III}$ mixed valence compounds. The results obtained are discussed with respect to the π acceptor properties of the bridge, the extent of metal−ligand orbital mixing and the relative back-donating properties of the metal centers. These results demonstrate the feasibility of controlling the extent of intercomponent communication by changing the identity of the metal centers and the oxidation state of the complex.

Introduction

Exploring the degree and mechanism of electronic interaction between two redox active metal centers, linked by a bridging ligand of well-defined structure, has been the subject of many experimental and theoretical investigations.[1] However, these previous investigations have predominantly focused on linking metal centers using bridges which do not have accessible redox state or linkers in which the metal-based redox processes proceed prior to bridge-based reactions. Electroactive bridging ligands offer the possibility of significant virtual coupling if the redox potentials of the bridge and redox centers are similar. Electron transfer via superexchange may be the dominant mechanism if the lowest unoccupied molecular orbital of the bridge is close in energy to donor and acceptor moieties, since the comparable energies of the bridge and metal redox centers act to reduce the activation barrier to electron tunneling. Redox active bridges create the possibility of modulating the degree of electronic coupling between the various molecular components since the electronic energy of both the bridge and its adjoining units will depend implicitly on the redox state of the bridge.

This contribution reports an investigation into these effects for homo- and heteronuclear ruthenium and osmium bisbipyridyl fragments bridged by O,N-coordination to 1,4-dihydroxy-2,5-bis(pyrazol-1′-yl)benzene (p-L) (Chart 1).

We focus on quinonoid or dioxolene bridges because their redox activity is preserved after binding metal centers. Therefore, depending on the relative values of the formal potentials, the metal centers may be linked by a quinone (Q), semiquinone (SQ), or hydroquinone (HQ), bridge. These states are expected to have significantly different structures and metal−ligand orbital interactions. In the literature, only very few dinuclear metal complexes based on 1,4-dioxelene ligands have been reported.[2] In previous studies, primarily ortho-chelating, 1,2-dioxolene ligands have been investigated. Unlike the system described here, a common feature of the previously investigated ligands is that the Ru(III) oxidation state is not stable for polypyridyl based complexes.[3] The hydroquinone bridge used in this work is expected to stabilize the Ru(III) oxidation state so that interaction across a quinone type bridge can be investigated.

We have investigated the electronic properties of these different redox states by performing electrochemical and spectroelectrochemical measurements. We expect that fundamental

* Corresponding author. E-mail: vosh@ccmail.dcu.ie. Fax: +353-1-7045503.

[†] Dublin City University.

[‡] The Queens University of Belfast.

(1) (a) Robin, M. B.; Day, P. Adv. *Inorg. Chem. Radiochem.* **1967,** *10*, 247. (b) Creutz, C. *Prog. Inorg. Chem.* **1983**, *30*, 1. (c) Ward; M. D. *Chem. Soc. Rev.* **1995**, 121. (d) Hage, R.; Haasnoot, J. G., Reedijk, J.; Vos, J. G. *Chemtracts-Inorg. Chem.* **1992**, *4*, 75. (e) Prassides, K., Ed. *Mixed Valency Systems*: *Applicaions in Chemistry, Physics and Biology*; Kluwer: Dordrecht, 1991.

(2) (a) Ernst, E.; Kasack, V.; Kaim, W. *Inorg. Chem.* **1988**, *27*, 1146. (b) Dei, A.; Gatteschi, D.; Pardi., L. *Inorg. Chem.* **1990**, *29*, 1442. (c) Joulie, L. F.; Schatz, E.; Ward, M. D.; Weber, F.; Yellowlees, L. J. *J. Chem. Soc., Dalton Trans.* **1994**, 799. (d) Hartl, F.; Snoeck, T. L.; Stufkens, D. J.; Lever, A. B. P. *Inorg. Chem.* **1995**, *34*, 3887.

(3) Metcalf, R. A.; Lever, A. B. P. *Inorg. Chem.* **1997**, *36*, 4762.

10.1021/ic980293l CCC: $15.00
Published on Web 10/10/1998

Chart 1

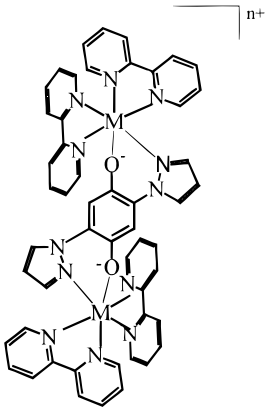

investigations focusing specifically on the role that electronic properties of the bridge play in dictating the extent of metal−metal and metal−ligand coupling will make it possible to design molecular systems that maximize electron-transfer efficiency.

Experimental Section

Chemicals. *cis*-$Ru(bpy)_2Cl_2 \cdot 2H_2O$, $Os(bpy)_2Cl_2 \cdot 2H_2O$, bpy-$d_8$, and 1,4-dihydroxy-2,5-bis(pyrazol-1′-yl)benzene were prepared as reported previously.[4−7] *p*-Benzoquinone was recrystallized from water and dried prior to use. Dioxan was dried by distillation over $LiAlH_4$ and was stored over activated molecular sieves (type 3A) prior to use. All other reagents (Aldrich) were used as received.

The metal complexes were purified using semipreparative HPLC system employing a model 353 Applied Chromatography Service pump and an ACS detector (model 353/UV−vis) together with a Magnum-9μ Partisil cation exchange column (1 cm × 25 cm). The mobile phase was acetonitrile/water (70:30 v/v) containing 0.15 M KNO_3 as eluent.

Absorption spectra were measured using a Shimadzu 3100 UV-vis/NIR spectrophotometer interfaced with an Elonex 486 PC. Electrochemistry was performed in either HPLC grade acetonitrile dried over activated molecular sieves (type 3A) or dimethylformamide (DMF) with 0.1 M tetraethylammonium tetrafluoroborate as the supporting electrolyte. Cells were of conventional design and were thermostated to within ±0.2 °C using a Julabo F10-HC refrigerated circulating bath. All potentials are quoted with respect to a BAS Ag/AgCl organic reference electrode, the potential of which was 45 mV more positive than that of the saturated calomel electrode (SCE). Under the conditions employed, the oxidation potential of ferrocene was +0.312 V vs Ag/AgCl. Cyclic voltammetry was performed using a CH Instruments model 660 Electrochemical Workstation. All solutions were degassed using nitrogen, and a blanket of nitrogen was maintained over the solution during all experiments.

Platinum microwires (Goodfellow Metals Ltd.) of radii between 5 and 25 μm sealed in soft glass as described previously.[8] Microdisk electrodes were exposed by removing excess glass using 600 grit emery paper followed by successive polishing with 12.5, 5, 1, 0.3, and 0.05 μm alumina. The polishing material was removed between changes of particle size by sonicating the electrodes in deionized water for at least 5 min. The polished electrodes were electrochemically cleaned by cycling in 0.1 M $HClO_4$ between potential limits chosen to first oxidize and then to reduce the surface of the platinum electrode. Finally, the electrode was cycled between −0.300 and 0.700 V in 0.1 M $NaClO_4$ until hydrogen desorption was complete.

Spectroelectrochemistry was carried out using a homemade Pyrex glass, thin-layer cell (1 mm). The optically transparent working electrode was a platinum gauze, which was inserted fully into the cell, the auxiliary electrode was a platinum wire, and the reference was Ag/AgCl; these were inserted into the sample reservoir on top of the cell. Experiments were carried out in dry, analytical-grade DMF containing 0.1 M tetraethylammonium tetrafluoroborate. The working electrode was held at the required potential throughout the measurement using an EG&G PAR model 362 scanning potentiostat. Absorption spectra were obtained on a Shimadzu 3100 UV/vis/NIR spectrophotometer interfaced with an Elonex PC-433 personal computer.

Resonance Raman spectra were recorded using an Ar^+ laser as the excitation source in the region of 351 to 528 nm, and a Ti-sapphire laser pumped by an Ar^+ laser for experiments carried out at wavelengths beyond 700 nm. A backscattering geometry was employed for the spectral accumulations using a liquid nitrogen cooled CCD multichannel detector coupled to a single stage monochromator (JY640HD). A holographic notch filter was used at the entrance slit to minimize Raleigh scattering. Resonance Raman spectra of electrochemically generated species were recorded using a cell fitted with an optically transparent platinum gauze electrode (62% transmittance) as working electrode. A silver wire was employed as a pseudoreference electrode and platinum wire as auxiliary. Tetrabutylammonium perchlorate (0.1 M in dry acetonitrile) was used as supporting electrolyte.[9]

Materials. $[(Ru(bpy)_2)_2(p\text{-}L)](PF_6)_2.KNO_3$ (RuHQRu). $[Ru(bpy)_2Cl_2] \cdot 2H_2O$ (0.676 g, 1.3 mmol) was dissolved in 40 cm^3 of ethanol/water (1:1 v/v) containing diethylamine (2%, v/v). This solution was deoxygenated with argon and heated, and p-L dissolved (0.15 g, 0.6 mmol) in 40 cm^3 of ethanol/water (1:1 v/v) (2% diethylamine) was added slowly over 20 min. The mixture was heated under reflux in an argon atmosphere for 4 h after which time the dark purple solution was reduced in volume to approximately 10 cm^3 and neutralized with sulfuric acid. After neutralization the solution was allowed to stand for several hours and then filtered to remove any salt formed. Saturated aqueous NH_4PF_6 was subsequently added to the solution, and the resulting purple precipitate was collected by filtration. The product contained approximately 5% mononuclear complex, which was removed by semipreparative HPLC. Yield 60%. Anal. Calcd for $Ru_2C_{52}H_{40}N_{13}O_5P_2F_{12}K$: C, 42.8; H, 2.6; N, 12.4. Found: C, 43.1; H, 3.1; N, 12.4. Presence of nitrate (from HPLC) was confirmed by FTIR. The analogue containing perdeuterated bpy was also prepared by this method.

$[Ru(bpy)_2(p\text{-}L)Os(bpy)_2](PF_6)_3 \cdot 6H_2O$ (RuSQOs). $[Os(bpy)_2Cl_2] \cdot 2H_2O$ (0.31 g, 0.5 mmol) was dissolved in 50 cm^3 of ethanol/water (70/30 v/v), with 2% diethylamine. The solution was deaerated with argon and heated to reflux. The mononuclear complex[2] $[Ru(bpy)_2(p\text{-}L)]^+$ (0.399 g, 0.5 mmol) dissolved in 10 cm^3 of ethanol was then added slowly to the reaction mixture over 30 min. The mixture was then allowed to reflux for 12 h. The volume of the solution was reduced to 10 cm^3, and 5 cm^3 of concentrated aqueous NH_4PF_6 was added. Subsequently, the resulting solid was collected by filtration and purified using HPLC as described above. Yield 86%. Anal. Calcd for $RuOsC_{52}H_{52}N_{12}O_8P_3F_{18}$: C, 36.3; H, 2.7; N, 9.8. Found: C, 35.9; H, 3.1; N, 8.2.

$[(Os(bpy)_2)_2(p\text{-}L)](PF_6)_3$ (OsSQOs). (OsOsSQ)was prepared using the same procedure described for (**RuHQRu**) except that $[Os(bpy)_2Cl_2] \cdot 2H_2O$ was used as the starting material. Yield 68%. Analysis calculated for $Os_2C_{52}H_{40}N_{12}O_2P_3F_{18}$: C, 37.0; H, 2.4; N, 10.0. Found: C, 36.7; H, 3.01; N,10.2.

Preparation of Mixed Valence Species. Mixed valence complexes were prepared either in situ by performing bulk electrolysis of solutions of the complexes dissolved in dry acetonitrile by holding the potential 100 mV positive of the second oxidation wave or by adding half an equivalent of cerium(IV) sulfate to the complex dissolved in acetonitrile.

(4) Sullivan, B. P.; Salmon, D. J.; Meyer, T. J. J. *Inorg. Chem.* **1978**, *17*, 3334.
(5) Lay, P. A.; Sargeson, A. M.; Taube, H.; Chou, M. H.; Creutz, C. *Inorganic Syntheses*; John Wiley and Sons: New York, 1983; Vol. 24.
(6) Keyes, T. E.; Weldon, F.; Muller, E.; Pechy, P.; Gratzel, M.; Vos, J. G. *J. Chem. Soc., Dalton Trans.* **1995**, 2705.
(7) Catalan, J.; Fabero F.; Guijarro, M. S.; Claramount, R. M.; Santa Maria, M. D.; de la Concepcion Foces-Foces, M.; Cano, F. H.; Elguero, J.; Sastre, R. *J. Am Chem. Soc.* **1990**, *112*, 747.
(8) (a) Faulkner, L. R.; Walsh, M. R.; Xu, C. *Contemporary Electroanalytical Chemistry*; Plenum Press: New York, 1990. (b) Xu, C. Ph.D. Thesis, University of Illinois at Urbana−Champaign, 1992. (c) Forster, R. J.; Faulkner, L. R. *J. Am. Chem. Soc.* **1994,** *116*, 5444.
(9) McNicholl, R. A.; McGarvey, J. J.; Al-Obaidi, A. H. R.; Bell, S. E. J.; Jayaweera, P. M.; Coates, C. G. *J. Phys. Chem.* **1995**, *99*, 12268.

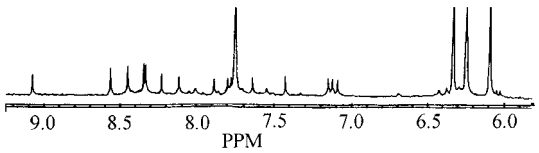

Figure 1. ^{1}H NMR (400 MHz) of [Ru(bpy-d_8)$_2$HQRu(bpy-d_8)$_2$]PF_6 in acetonitrile-d_3.

In general, the chemical method was inferior, as the mixed valence states under these conditions were rarely stable for more than 30 min.

Results and Discussion

Structural Characterization. In trying to understand those factors that control electronic coupling across redox active bridges, it is essential to first determine the composition of the compounds obtained. This is particularly important in the present case since the oxidation states of dioxolene-containing compounds have been the subject considerable debate. Therefore, ^{1}H NMR spectroscopy was performed to elucidate the binding mode and structure of the complexes. However, the complexity of the spectra makes it difficult to unambiguously assign all of the observed resonances. To simplify these spectra, and to gain a more definitive insight into the binding mode, **RuHQRu** containing perdeuterated bipyridyl ligands was synthesized. Deuteration of the bipyridyl ligands represents a powerful method of elucidating the ^{1}H NMR of complex spectra since it eliminates, or reduces to singlets, all resonances associated with the bpy ligands (Figure 1). Significantly, well-defined resonances are obtained for the ruthenium dinuclear complexes even under neutral conditions, indicating the diamagnetic nature of **RuHQRu** and the absence of a semiquinone bridge in this compound. The inherent symmetry of this complex is reflected in its proton NMR spectrum.[10] Only one (2H) resonance is observed for each pyrazole proton, H^3 at 6.4 ppm (free ligand 7.78 ppm), H^4 appears as a triplet at 6.3 ppm (free ligand 6.57 ppm), and H^5 appears as a doublet at 7.9 ppm (8.24 ppm in the free ligand). One singlet is observed for the hydroquinone bridge at 6.1 ppm (7.27 ppm free ligand). In each instance, the resonances are shifted significantly upfield in comparison with the free ligand, particularly for the hydroquinone moiety. As the HQ ligand is largely incapable of accepting back-donated electron density, the upfield shifts are attributed to the negative charges on the hydroxylate moieties. Attempts to study the ^{1}H NMR of the deprotonated free ligand failed because the semiquinone species forms spontaneously on adding base. ^{1}H NMR spectra of the osmium-containing complexes are broadened and therefore inadequate for detailed structural assignment. This is attributed to the presence of semiquinone in the products obtained and confirmed by the elemental analysis of these complexes, from which it is apparent they possess a 3+ charge, not the anticipated 2+ as observed for the ruthenium dimer.

General Electrochemical Properties. The electrochemical data obtained for the complexes are listed in Table 1. Figure 2 illustrates the voltammetric response obtained for **RuHQRu**. The electrochemical response shown is typical of that observed for each of the dinuclear complexes in that six distinct redox processes are observed between ±2 V. For each of the redox couples, irrespective of the complex in question, the difference between the anodic and cathodic peak potentials, ΔE_p, is between 65 and 90 mV at a scan rate, υ, of 5 V s^{-1}. For scan rates above 5 V s^{-1}, for each of the complexes the anodic and cathodic peak currents are equal to within experimental error and increase linearly with $\upsilon^{1/2}$. These observations are consistent with electrochemically reversible reactions occurring under diffusion control. Moreover, that reversible responses are observed at relatively high scan rates indicates that the rate of heterogeneous electron transfer across the electrode/solution interface is relatively rapid. With the exception of the mixed metal complex which integrates for four electrons, voltammetry and bulk electrolysis show that the processes observed at negative potentials are two-electron processes. The redox processes observed at positive potentials involve the transfer of a single electron.

In each complex, the first three oxidation processes observed at positive potentials are reversible for $0.5 \le \upsilon \le 50$ V s^{-1}. However, the reversibility of the fourth oxidation step depends on the scan rate, and the reactions are irreversible at long experimental time scales. This behavior is not consistent with slow interfacial electron transfer but suggests that the oxidized product undergoes a subsequent chemical reaction. The lower scan rate limit at which reversibility is observed depends on the identity of the metal. Consistent with its greater reactivity, the redox process was reversible at scan rates greater than 5 V s^{-1} for the ruthenium complex, while for osmium scan rates greater than 1 V s^{-1} were sufficient to observe reversible responses.

The well-behaved, mostly reversible, electrochemistry observed makes these dinuclear, dioxolene-based systems attractive models for investigating electronic coupling between metal centers and between metal centers and the bridge.

The voltammetric responses show that the first two oxidations do not change systematically with the identity or number of metal centers bound to the bridge. This observation indicates that the electrochemistry observed is primarily associated with the bridge and that electronic communication across the reduced form of the bridge is weak. This conclusion is supported by analyzing the bipyridyl reductions (*vide infra*). It is also worth noting that the stabilization of the semiquinone state is considerable. To quantify the extent of this stabilization comproportionation constants K_c can be employed, which are defined as $K_{c(SQ)}$ for the ligand-based process;

$$2SQ \overset{K_{c(SQ)}}{\rightleftharpoons} Q + HQ \qquad (1)$$

and as $K_c(M)$ for the metal-based redox processes

$$2[M^{III}-Q-M^{II}] \overset{K_{c(M)}}{\rightleftharpoons} [M^{II}-Q-M^{II}] + [M^{III}-Q-M^{III}] \qquad (2)$$

Comproportionation constants were obtained using eq 3, where $\Delta E°$ is the potential difference between the two redox processes observed for the ligand and metal center, respectively.

$$\mathrm{Log}_{10}(K_c) = (\Delta E°/0.059\ \mathrm{V}) \qquad (3)$$

In contrast to the ill-defined two-electron oxidation observed for the Ru monomer[11] and the single 2-electron oxidation observed for the free ligand, oxidation of the dioxolene bridge for **RuHQRu** proceeds in two well-resolved, reversible, one-electron steps at 0.130 and 0.545 V vs SCE. $K_{c(SQ)}$ for **RuSQRu** is approximately 8.6×10^6, emphasizing the large degree of stabilization of the semiquinone state. Similar large stabilization of semiquinone has been observed by Lever and co-workers for mononuclear catechol (1,2-dioxolene) com-

(10) See Supporting Information (S1).

(11) Keyes, T. E.; Jayaweera, P. M.; McGarvey, J. J.; Vos, J. G. *J. Chem. Soc, Dalton Trans.* **1997**, 1627.

(12) Griffith, W. P. *Trans. Met. Chem.* **1993**, *250*, 18 and references therein.

Table 1. Redox Potentials and Comproportionation Constants (K_c) for Ligands and Metal Centers[a]

	redox potentials[a] (V vs SCE)			K_c	
complex	p-L	bpy	metal	ligand	metal
RuHQ	0.29, 0.39	−1.52, −1.72	1.26	50	
RuRuHQ	0.13, 0.54	−1.51 (2e⁻), −1.66 (2e⁻)	1.32, 1.64 (irr)	8.9×10^6	2.7×10^5
RuOsHQ	0.19, 0.44	−1.62 (4e⁻)	1.01, 1.75 (irr)	1.7×10^4	3.5×10^{12}
OsHQ	0.18, 0.52	−1.61, −1.7	1.03	5.6×10^5	
OsOsHQ	0.23, 0.42	−1.63 (2e⁻), −1.88 (2e⁻)	0.98, 1.58 (irr)	1.6×10^3	1.5×10^{10}

[a] One-electron steps except where otherwise stated.

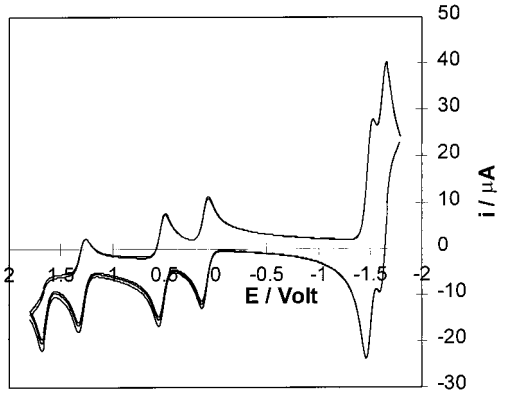

Figure 2. Electrochemistry of **RuHQRu** in DMF containing 0.1 M TBAF, scan rate 0.1 V/s.

plexes,[12] where under neutral conditions semiquinone is often the most stable species.

Semiquinone stabilization occurs to a lesser degree in the osmium-containing dinuclear complexes, the $K_{c(SQ)}$ values being 1.7×10^4 and 1.6×10^3 for the **RuSQOs** and **OsSQOs** complexes, respectively. The redox potentials in Table 1 suggest that the HQ state of the bridge is somewhat stabilized by osmium while ruthenium stabilizes the SQ state.

Since metal-based redox reactions were either outside of the accessible potential window, or were irreversible, earlier reports addressing the electrochemical properties of dioxolene complexes, focused on the redox reactions of the bridge without explicit attention to the nature and extent of metal−metal interactions across the oxidized bridge.[2,3] In the systems described here, the metal-based redox reactions occur at potentials that are positive of the bridge-based redox processes but remain within an easily accessible potential window. Thus, these complexes open up an important new avenue of investigation, that of quinone-mediated metal−metal communication in dinuclear structures.

Delocalization, electrostatics, asymmetry, and statistical effects are expected to make the formal potentials of the two metal centers different from one another even when they are structurally identical.[1] Moreover, where the bridging ligand is a π acceptor, inductive effects are also anticipated to play a role.[13] Table 1 shows that large $K_{c(M)}$ values are observed for all complexes, indicating that there is always substantial intermetal communication across the quinone bridge. The magnitude of $K_{c(M)}$ clearly depends on the identity of the metal centers with $K_{c(M)}$ for **OsQOs** being 5 orders of magnitude greater than for the Ru analogue. The ruthenium/osmium mixed metal complex exhibits a $K_{c(M)}$ value of 3.5×10^{12}. It is possible to quantify the contribution from the coordination asymmetry to the observed $K_{c(M)}$ value by comparing the oxidation potentials of the ruthenium and osmium monomers. After correcting for this difference in formal potential, $K_{c(M)}$ for the **RuQOs** complex is approximately 4.4×10^8. Thus, the degree of stabilization in terms of delocalization/induction for the heteronuclear complex lies midway between that found for the ruthenium and osmium homonuclear complexes.

For the Creutz−Taube complex, the best known example of a low π^* ligand bridge, a similar trend was observed, with $K_{c(M)}$ of the osmium complex greater by approximately 6 orders of magnitude than that of ruthenium.[1b] Similar trends have also been observed previously in other bridging ligands with low-lying π^* levels bound to osmium[14] and is related to the π back-acceptor properties of the osmium center. Closer energy matching of quinone (π^*) and Os orbitals and stronger π interaction lead to a larger electronic drain on the quinone bridge, resulting in a higher value for $K_{c(M)}$. Therefore, the large $K_{c(M)}$ in these complexes may be attributed to delocalizational interactions between the metal centers, a consequence of metal−ligand orbital mixing and, especially important, an inductive contribution attributable to the low-energy π^* nature of the bridge, which is manifested by the trend in the magnitude of $K_{c(M)}$ as the identity of the metals changes. After the oxidation of the first metal, the π acidity of the bridge increases and the remaining metal center is forced to higher potential as a result of this electronic drain.

It is not possible to directly probe the extent of metal−metal communication across the hydroquinone bridge, as the hydroquinone electrochemistry precedes that of the metals. However, the redox behavior of the bipyridyl groups provides valuable insight into coupling across the reduced bridge. What is striking about the bipyridyl reactions of the homonuclear complexes is that each reduction step is a single, reversible two-electron wave. Comparison with the appropriate mononuclear complexes reveals that the reduction potentials of bipyridyl units attached to the same metal differ by at least 100 mV. This reveals that, as expected, each bipyridyl reduction under the two-electron wave for the dimers occurs at the different metal sites. Moreover, the presence of a reduced bipyridyl radical at one metal site has no influence on the reduction potential of the bipyridyl at the other metal site. The second set of bipyridyl reductions behave in an identical fashion, appearing as single two-electron waves. In sharp contrast, splitting of the bpy reductions is observed for dinuclear complexes based on the ligand 3,5-bis(pyridin-2-yl)1,2,4-triazole,[15] where metal interaction across the deprotonated triazolate bridge is known to be strong. The absence of resolution in the bipyridyl reductions described here seems to suggest lack of significant coupling over the HQ bridge. This behavior suggests that the two negative charges present on the HQ, more than likely on the

(13) (a) Sutton, J. E., Sutton. P. M.; Taube, H. *Inorg. Chem*. **1979**, *18*, 1017. (b) Sutton, J. E.; Taube, H. *Inorg. Chem*. **1981**, *20*, 3125.

(14) (a) Denti, G.; Campagna, S.; Sabatino, L.; Serroni, S.; Ciano, M.; Balzani, V. *Inorg. Chem*. **1990**, *29*, 4750. (b) Kalyanasundaram, K.; Nazeeruddin, Md. K. *Inorg. Chim. Acta* **1994**, 226, 213 and references therein.

(15) Hage, R.; Haasnoot, J. G.; Stufkens, D. J.; Snoeck, T. L.; Vos, J. G.; Reedijk, J. *Inorg. Chem*. **1989**, *28*, 1413.

Table 2. Electronic Properties of Compounds Reported in the Various Oxidation States

complex	wavelength (nm) (ϵ)	assignment of optical transition
RuHQ	490 (5754)	Ru(dπ)−bpy(π*), MLCT
	578	p-L($3b_1$)−bpy(π*1), ILCT
RuQ	416	Ru(dπ)−bpy(π*), MLCT
	701	Ru(dπ)−p-L(quinone)($3b_1$), MLCT
RuRuHQ	490 (8300)	Ru(dπ)−bpy(π*), MLCT
	573	p-L($3b_1$)−bpy(π*1), ILCT
RuRuSQ	456	Ru(dπ)−bpy(π*), MLCT
	1290 (4807)	Ru(dπ)−p-L(SQ)($3b_1$), MLCT
RuRuQ	392	Ru(dπ)−bpy(π*), MLCT
	764 (sh)	Q($3b_1$)−bpy(π*1), ILCT
	1006 (20 750)	Ru(dπ)−p-L(Q)($3b_1$), MLCT
$Ru^{II}QRu^{III}$	380	Ru(dπ)−bpy(π*), MLCT
	994 (3709)	Q($3b_1$)−bpy(π*1), ILCT
	2104 (v.w.)	Ru^{II}(dπ)−Ru^{III}(dπ), IVCT
OsOsHQ	500 (6710)	Os(dπ)−bpy(π*), MLCT
	580 (sh)	p-L($3b_1$)−bpy(π*1), ILCT
	750 (2164)	Os(dπ)−bpy($^3\pi$*), ^{3}MLCT
OsOsSQ	480	Os(dπ)−bpy(π*), MLCT
	750	Os(dπ)−bpy($^3\pi$*), ^{3}MLCT
	1062 (549)	Os(dπ)−SQ($3b_1$), MLCT
	2300 (887)	Os(dπ)− SQ($3b_1$), ^{3}MLCT
OsOsQ	454	Os(dπ)−bpy(π*), MLCT
	750	Os(dπ)−bpy($^3\pi$*), ^{3}MLCT
	924 (2896)	Os(dπ)−Q($3b_1$), MLCT
$Os^{II}QOs^{III}$	400	Os(dπ)−bpy(π*), MLCT
	920	Os(dπ)−Q($3b_1$), MLCT
	1132 (v.w.)	Os^{II}(dπ)−Os^{III}(dπ), IVCT
RuOsHQ	500 (7900)	Os/Ru(dπ)−bpy(π*), MLCT
	590	p-L($3b_1$)−bpy(π*1), ILCT
	750 (1571)	Os(dπ)−bpy($^3\pi$*), ^{3}MLCT
RuOsSQ	438 (6143)	Os/Ru(dπ)−bpy(π*), MLCT
	1156 (2665)	Os/Ru(dπ)−SQ($3b_1$), MLCT
	1980 (1796)	Os(dπ)−SQ($3b_1$), ^{3}MLCT
RuOsQ	390 (5699)	Os/Ru(dπ)−bpy(π*), MLCT
	770	Os(dπ)−bpy($^3\pi$*), ^{3}MLCT
	1018 (10 424)	Ru(dπ)−Q($3b_1$), MLCT
	1854 (929)	Os(dπ)−Q($3b_1$), ^{3}MLCT
$Ru^{II}QOs^{III}$	364	Os/Ru(dπ)−bpy(π*), MLCT
	756 (3122)	Os(dπ)−bpy($^3\pi$*), ^{3}MLCT
	990 (2331)	Ru(dπ)−Q($3b_1$), MLCT

oxygen atoms, in effect screen the metal centers from each other rather than promote communication.

Each of the bipyridyls for **RuHQOs** undergo a single electron transfer step at essentially the same potential (independent of scan rate) and this is attributed to the asymmetry of the complex induced by the dissimilar metals. Again, absence of resolution of the individual redox steps is attributable to inefficient M−M communication.

Spectroelectrochemistry. To obtain further information about the nature of redox changes UV/vis and resonance Raman spectroscopy have been carried out. These techniques can yield important information about the effect of changes in the redox composition of the compounds on electronic coupling and electron distribution. For example, the relative direction and magnitude of the shifts observed in the metal-to-ligand charge transfer (MLCT) bands observed as the bridge is selectively oxidized reveal the tendency of the different metal centers to back-donate electron density to the bridge and thereby stabilize the metal t_{2g} levels. Furthermore, the bandwidths, energies and solvent dependence of the spectral features evolving with each oxidation step are valuable probes in determining the extent of coupling of sites from which the transitions originate.

A detailed listing of the UV/vis properties of the various redox states on the complexes is given in Table 2. As Table 2 reveals, the complexes discussed exhibit rich spectral responses to variation in the applied potential. Figure 3 shows the electronic

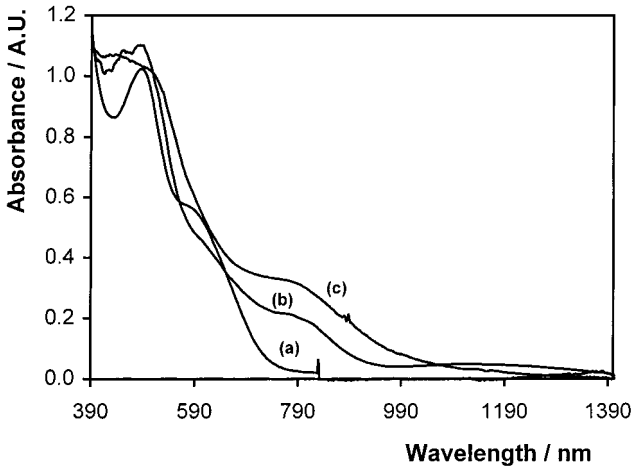

Figure 3. Absorption spectra of (a) **RuHQRu**, (b) **RuHQOs**, and (c) **OsHQOs** in acetonitrile containing 0.1 M TEAP, at −0.2 V vs SCE.

spectra of the three dinuclear complexes where the bridge is in its reduced state. To ensure complete reduction of the osmium-containing complexes, spectra were recorded at −0.2 V (vs Ag/AgCl). For **RuHQRu** three distinct spectral features are observed at 380, 490, and 578 nm. **RuHQRu** and **OsHQOs** show similar absorption spectra with an intense MLCT band around 500 nm, a shoulder around 580 nm, and a low-intensity feature around 750 nm. In each compound, the high-energy transitions (380−500 nm) are attributed to Ru or Os(dπ)−bpy(π*) MLCT transitions. The 580 nm shoulder is assigned to a HQ(π)−bpy(π*) interligand charge transfer by comparison with $[Ru(bpy)_2(p\text{-}L)]^+$ and because of the fact that this transition disappears after the first oxidation. The low-energy (750 nm) band in the complexes containing Os is attributed to Os (dπ) bpy($^3\pi$*) singlet-to-triplet transition by comparison with other osmium complexes[16,17] and because of the fact that it is observed throughout the first two, bridge-based oxidation steps.

Oxidation of RuHQRu. Figure 4 shows that, in a fashion similar to its mononuclear analogue, after the first oxidation of **RuHQRu** the Ru(dπ)−bpy(π*) MLCT band shifts to a shorter wavelength and the shoulder at 580 nm disappears. These two observations confirm the ligand-based nature of the first redox step.

Concomitantly, an intense and extremely broad feature appears in the NIR region centered around 1290 nm (in DMF). Both its half-width and peak position are strongly solvent dependent. For example, in acetonitrile, this band occurs at 1316 nm (ϵ = 4807 M^{-1} cm^{-1}) full width at half-maximum (fwhm) $\Delta\nu_{1/2}$ = 4112 cm^{-1}, whereas in dichloromethane, the band shifts to higher energy and is located at 1260 nm (ϵ = 8338 M^{-1} cm^{-1}) with a fwhm of 3154 cm^{-1}. Kaim and co-workers[4a] have assigned a similar feature in related complexes to a transition from a Ru^{II}dπ level to a semiquinone based singly occupied molecular orbital (SOMO). Lever et al. reported a similar transition at 925 nm in a mononuclear semiquinone complex bound to catechol ligands.[18] We therefore attribute the 1260 nm band to a Ru^{II}(dπ)−SQ(SOMO) MLCT occurring within a valence-trapped species. Our justification for the

(16) (a) Schanze, K. S.; Neyhart, G. A.; Meyer, T. J. *J. Phys. Chem.* **1986** **90**, 2182. (b) Hupp, J. T.; Neyhart, G. A.; Meyer, T. J. *J. Am. Chem. Soc.* **1986**, 108, 5349.
(17) Kober, E. M.; Goldsby, K. A.; Narayana, D. N. S.; Meyer, T. J. *J. Am. Chem. Soc.* **1983**, *105*, 4304.
(18) (a) Haga, M.; Dodsworth, E. S.; Lever, A. B. P. *Inorg. Chem.* **1986**, *25*, 447. (b) Masui, H.; Lever, A. B. P.; Auburn, P. R. *Inorg. Chem.* **1991**, *30*, 2402.

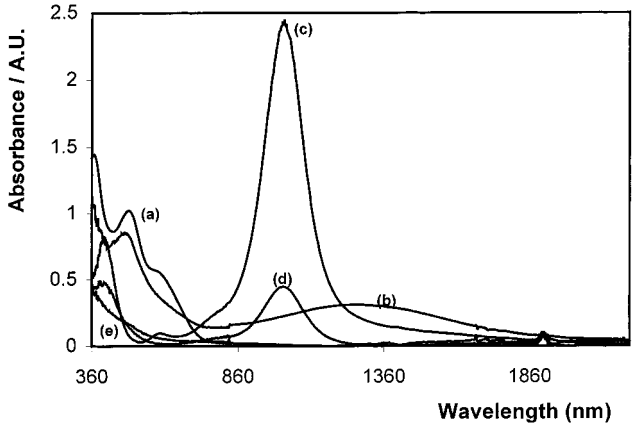

Figure 4. Spectroelectrochemistry of **RuHQRu** in DMF containing 0.1 M TBAF; (a) 0 V, (b) 0.3 V, (c) 0.8 V, (d) 1.6V, (e) 1.8 V vs Ag/AgCl.

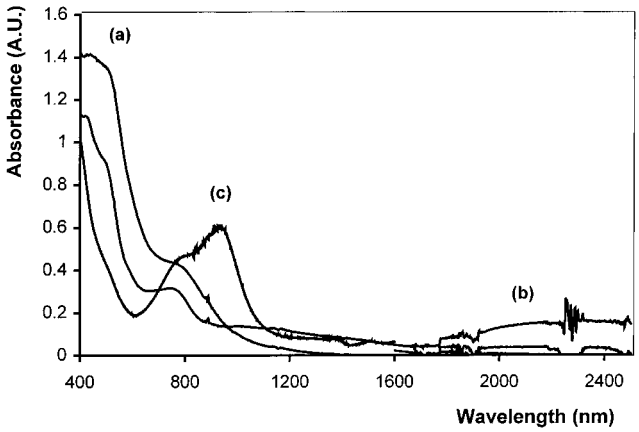

Figure 5. Spectroelectrochemistry of **OsHQOs** in DMF containing 0.1 M TBAF; (a) −0.2 V, (b) 0.2 V, (c) 0.6 V vs Ag/AgCl.

assumption of a valence trapped species is that this band is remarkably broad indicating weak resonant mixing of the bridge and metal-centered orbitals. In other reports of metal-to-semiquinone transitions, strong ligand−metal mixing occurs, and this band is narrow.[19] Band broadness is associated with a large vibrational (or Franck−Condon) barrier to the electron transfer, since fwhm is proportional to the Franck Condon factor to the power of a half. In a valence trapped species, the Ru(II) to SQ transition will result in a charge separated state consisting of Ru(III) and HQ, therefore considerable nuclear reorganization will be associated with this transition accounting for its large width. Furthermore, the energy and intensity of the transition are very sensitive to the identity of the solvent, suggesting solvent stabilization of a charge separated species. Such a strong solvent dependence is observed for transitions in related charge-transfer complexes and is not consistent with the strong resonant mixing required for a $\pi-\pi^*$ transition in a delocalized system.

After the second oxidation step, the feature at 1260 nm disappears and is replaced by a sharp and extremely intense (ϵ = 20 750 M^{-1} cm^{-1}) absorbance at 1006 nm. The characteristics of this feature are similar to that observed in the mononuclear complex in the same redox state (**RuQ**), albeit of lower intensity in the latter. Therefore, this band is attributed to a $Ru^{II}d\pi-Q(\pi^*)$ MLCT process. This intense and narrow feature exhibits only a very slight solvent dependence (10 nm between acetonitrile and dichloromethane), which suggests that considerably more mixing occurs between the metal and quinone orbitals, than for the semiquinone. This occurs despite the greater energy difference between the metal and ligand orbitals in the quinone compared to the semiquinone (as manifested by the higher energy MLCT in the former) and may be attributed to the strongly π accepting nature of the quinone ligand.

Oxidation of the first metal center reduces the intensity of the 1006 nm band to one-sixth its initial intensity and shifts the band to 994 nm; the MLCT located at 420 nm also decreases in intensity. A weak transition is observed at 2100 nm, which is tentatively assigned to an intervalence charge-transfer process. The spectral changes were reversible for the processes located on the bridge and first metal center. However, oxidizing the solution at 1.6 V gave irreversible responses and the formation of a yellow product with λ_{max} at 420 nm which was not further identified.

Oxidation of OsHQOs. Figure 5 shows the spectral changes when **OsHQOs** is selectively oxidized in DMF. The electronic features observed are in agreement with those observed for the ruthenium dinuclear complex. MLCT bands at about 500 and 750 nm are maintained in the spectra until after the last oxidation process and confirm that for this compound the first two redox processes are bridge based. When the potential is held at 0.2 V, two broad, weak bands appear at approximately 1100 and 2400 nm. The low intensity of these spectral features contrast with those observed for **RuSQRu** where spectral features are intense; however, their solvent dependence is similar. Similarly to the ruthenium complex, these transitions are attributed to Os(II) to semiquinone charge-transfer transitions.

The appearance of the lower energy transition at 2400 nm is not completely understood, but we believe it to be due to splitting of the nominally degenerate Os 5dπ orbitals, a consequence of strong spin−orbit coupling due to the heavy Os center and asymmetry induced by the radical state of the bridge.[20] The presence of a similar low-energy transition in the osmium−semiquinone monomer precludes any contribution from intervalence charge transfer.[21] We believe this to be among the lowest energy MLCT transitions reported to date for an Os(II) species.

At 0.4 V the weak, broad absorbances in the near-infrared are lost, and an intense new feature appears at 890 nm. This band is attributed to $Os^{II}d\pi-Q(\pi^*)$ MLCT transition. The greater blue shift in this feature compared with the equivalent transition in **RuQRu** may be attributed to greater stabilization of the Os(II) t_{2g} level when bound to the strongly π accepting quinone as a result of this metals greater propensity for π back-donating. However, the lower intensity and greater fwhm of this feature compared with the Ru analogue suggest considerably less delocalization is occurring.

After oxidizing the first metal, both the feature at 890 nm and the Os to bpy MLCT are reduced in intensity. There is some evidence for the formation of a very weak feature around 1700 nm which we tentatively assign as the intervalence charge-transfer transition. Throughout the first three oxidation steps of **OsHQOs** the band at 750 nm remains largely unchanged, beyond some changes in intensity. That this ^{3}MLCT transition persists through the first three oxidation steps further confirms that it is the bridging ligand and not the osmium metal that is being oxidized.

Oxidation of RuHQOs. Figure 6 illustrates the spectroelectrochemical responses observed for the mixed metal com-

(19) Hartl, F.; Snoeck, T. L.; Stufkens, D. J.; Lever, A. B. P. *Inorg. Chem.* **1995**, *34*, 3887.
(20) Lever, A. B. P. *Inorganic Electronic Spectroscopy*; Elsevier Science Publishers B.V.: Amsterdam, 1984.
(21) Unpublished results.

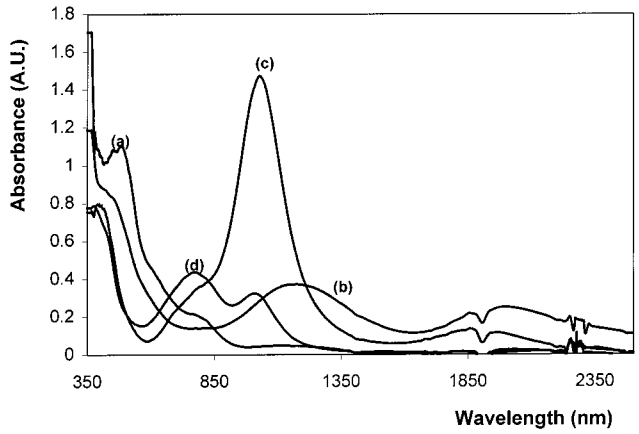

Figure 6. Spectroelectrochemistry of **RuHQOs** in DMF containing 0.1 M TBAF; (a) −0.2 V, (b) 0.15 V, (c) 0.9 V, (d) 1.3 V vs Ag/AgCl.

plex, **RuHQOs** in DMF. Again the ruthenium and osmium MLCT features are maintained in the spectra until the last oxidation process. After the initial one-electron oxidation, two broad and intense features appear at 1156 and 1980 nm. The spectrum of the heteronuclear complex appears to consist of a superposition of the properties the analogous homonuclear complexes. The bands at 1156 and 1980 nm are therefore ascribed to the overlay of $Ru^{II}d\pi-SQ(SOMO)$ and $Os(II)(d\pi)-SQ(SOMO)$ transitions. These results imply that the system is essentially valence trapped. This result contrasts strongly with other ligands in the semiquinone state where mixing is observed to be extensive and valence trapping is small.

After the second oxidation process, the 1156 nm band is lost and replaced by a narrow and intense feature at 1018 nm, which possesses a shoulder at approximately 770 nm. This 1018 nm band is highly reminiscent of that observed for RuQRu and shows only a very small solvent dependence. Although its extinction coefficient is approximately 50% lower that found in the mononuclear ruthenium complex **RuQ**, spectral similarities suggest that this band is also attributed to a Ru^{II}−quinone MLCT with strong mixing at the quinone−ruthenium center. The analogous osmium based transition, which is much weaker in the osmium complex is probably obscured by the high-intensity Ru^{II}−quinone transition and probably contributes to the intensity of the shoulder at 770 nm. The MLCT band at 490 nm blue shifts to 430 nm and is further reduced in intensity at this potential. The band at 1980 nm is reduced in intensity and shifted to 1854 nm. This transition had been assigned as $Os^{II}(d_{xy})-SQ(SOMO)$ (MLCT) from a nondegenerate Os(dp) orbital. Its continued presence in **RuQOs** is attributed to strong delocalization of electronic density between the quinone and ruthenium center. The delocalization of the Ru(II) center alters the character of the bridge from a purely quinone bridge to a mixed quinone/semiquinone state, making this MLCT transition possible, albeit at higher energy and with lower intensity.

After oxidation at 1.1 V the 1854 nm band is lost and the feature at 1026 nm is reduced significantly in intensity and shifted to 990 nm. A very weak new feature evolves at 1880 nm, and all these features are lost irreversibly on application of potentials greater than 1.7 V. In line with the electrochemistry and resonance Raman data (below) at 1.1 V the osmium is anticipated to be oxidized first. Disappearance of the ^{3}MLCT transition at 740 nm appears to confirm this. The feature at 990 nm is therefore attributed to the Ru(II)−Q MLCT transition as observed in **RuQ** and **RuQRu**. The feature at 756 nm is tentatively assigned to a metal−metal charge transfer between the Ru(II) and Os(III).

The considerable reduction in intensity of the 1026 nm band on oxidation of the osmium is also significant. It implies that substantial perturbation occurs at the quinone center on osmium oxidation, which is suggestive of strong M−quinone coupling.

In summary, these results suggest that when the ligand is in the quinone state considerable metal−ligand orbital mixing occurs, particularly between ruthenium and quinone, where appreciable resonance delocalization of the metal electron density occurs across the ligand. In each instance M−L mixing is substantially greater for the quinone than the semiquinone bridge, this is in direct contrast to other reported systems where invariably M(II) delocalization with the SQ state is always significantly stronger than in quinone system. The reason for this different behavior is at present unclear, but we are currently working on computational studies of these complexes in order to elucidate this apparent anomaly.

The very low intensity of the transitions ascribed to intervalence electron transfers implies the large $K_{c(M)}$ values obtained from electrochemical measurements does not arise because of delocalizational effects. We believe that a substantial component of $K_{c(M)}$ is derived from the inductive effects caused by the strong π accepting nature of the electron-poor quinone bridge.

Resonance Raman Spectroscopy. The electrochemical and UV/vis data presented above strongly suggest that the bridge is oxidized before the metal centers. To further substantiate these assignments, we have carried out resonance Raman experiments at 632.8 and 457.9 nm (He:Ne laser), thereby monitoring for the presence of the $M(II)(d\pi)-bpy(\pi^*)$ transitions. These transitions are taken as markers for the presence of M(II) centers.[22,23]

Figure 7a−c shows the resonance Raman spectra for the homonuclear ruthenium complex excited at 457.9 nm after bulk electrolysis at 0, 0.2, and 0.6 V, respectively. As with other reported MLCT bands of this nature, marker vibrations for bpy[22,23] are evident at 1605, 1558, 1486 1318, 1268, and 1172 cm^{-1}. That these bands shift to 1576, 1529, 1430, 1343, 1256, and 1003 cm^{-1} upon deuteration of the bipyridyl ligands confirms this assignment. The first and second oxidation steps do not significantly alter these Raman features apart from changes in the relative ordering of the intensities. These changes in intensity arise from the blue shift of the MLCT band causing this transition to become preresonant with the laser excitation. UV/vis spectroelectrochemistry shows that the MLCT band at 490 nm shifts to 469 and then to 411 nm after the first and second oxidation steps, respectively (Figure 7, inset). Therefore, consistent with the electrochemical data presented above, resonance Raman spectroscopy confirms that the first two oxidations are based on the 1,4-dioxolene bridge in this system. Moreover, in agreement with the behavior reported previously for the mononuclear species and the free hydroquinone ligand,[2] when the bridge is in the reduced form, a vibration is observed at 1342 cm^{-1}. This band disappears after the first oxidation process, further confirming that the first oxidation process is based on the bridge.

The resonance Raman spectrum was also recorded with excitation at 632.8 nm to confirm the nature of the low-energy absorbance centered around 580 nm. In the high-energy region, bands at 1604, 1556, 1482, 1317, 1265, 1168, and 1012 cm^{-1}

(22) Mabrouk, P. A.; Wrighton, M. S. *Inorg. Chem.* **1986**, *25*, 526.
(23) Strommen, D. P.; Mallick, P. K., Danzer, G. D.; Lumpkin, R. S.; Kincaid, J. R. *J. Phys. Chem.* **1990**, *94*, 1357.

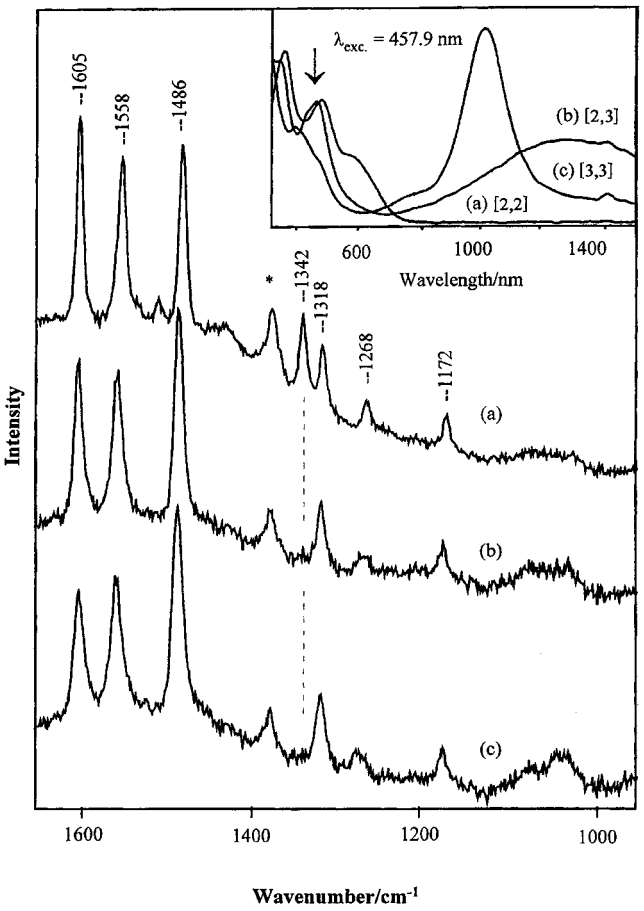

Figure 7. Resonance Raman of **RuHQRu** (λ_{ex} = 457.9 nm), in acetonitrile containing 0.1 M TBAF, (a) before oxidation, (b) after the first one-electron oxidation, and (c) after second one-electron oxidation step. Spectraelectrochemistry of **RuHQRu** at different oxidation states in the same solvent.

are observed; these are values typical of bipyridyl vibrations, and, as expected, they are shifted by between 30 and 60 cm^{-1} on bipyridyl deuteration. The low-energy features observed at 671, 648, 568, and 482 cm^{-1} are insensitive to bipyridyl deuteration and are associated with Ru−O and bridge-coupled modes. This 580 nm transition disappears after the first oxidation step, and is assigned to a hydroquinone-to-bipyridyl interligand charge transfer.[19]

The above discussion applies to all three dinuclear complexes. The overall intensity and signal-to-noise ratio of the spectra are lower for the osmium than for the ruthenium analogues. However, all bpy-based bands remain evident after both oxidation steps, confirming that as, for the ruthenium analogues, the first oxidation steps are bridge and not metal based. Thus, Raman spectra of these complexes confirm that despite the less positive redox potential of the osmium polypyridyl fragment, is not possible to generate an Os^{III}/Ru^{II} or Os^{III}/Os^{II} mixed valence compound across the reduced 1,4-dihydroxy-2,5-bis-(pyrazol-1′-yl)benzene bridge.

Conclusions

These investigations into homo- and, for the first time, heteronuclear ruthenium and osmium complexes linked by a redox active 1,4-dioxolene bridge are revealing of the subtle effects that changing symmetry, electron density, and oxidation states has on electronic coupling within the complex. Electrochemistry, spectroelectrochemistry, and resonance Raman data all confirm that the first two oxidation processes are based on the bridge for each of the complexes investigated, regardless of the nature of the metal. This fact, coupled with the relative potentials of the further oxidation process, which show trends consistent with the periodicity of the metals involved, confirms that the third and fourth oxidation processes are metal based. Comparison of the spectroscopic properties of the complexes with each other, their mononuclear analogues, and other relevant species suggests that these systems possess a gradient of resonant mixing of metal and ligand orbitals across the oxidation range of the bridging ligand. We observe that the M−L mixing increases in the order HQ ≪ SQ < Q. Using the bipyridyl reductions as probes, we find minimal intermetal communication and metal bridge mixing in the hydroquinone state. A rich optical spectroscopy reveals moderate (although significantly less than reported for comparable systems) mixing of M bridge states in the semiquinone state, with extensive mixing of M and L orbitals for the quinone state. This effect is particularly strong for the ruthenium dinuclear complex and is in marked contrast to other systems where, despite stronger quinone π acidity, the SQ state exhibits strongest metal−ligand mixing. $K_{c(M)}$ values are indicative of strong intermetal communication across the quinone bridge, which are of the order RuRu < RuOs < OsOs, however, very weak intervalence transitions suggest that the most important contribution to $K_{c(M)}$ may be derived from the inductive effect of the low-lying π^* orbitals and the trend is due to the varying π donating ability of the metals.

This work serves to illustrate how manipulation of metal sites and dioxolene oxidation states may be used to modulate the occurrence and extent of intercomponent interactions in a supramolecular system. Such issues are potentially important in the field of molecular electronics where controlling the redox accessibility and reversibility of electron-transfer processes is vital. These characteristics, along with the rich electrochromicity of these complexes, may be further modulated by manipulation of counterligands and the σ donor and π acceptor properties of coordinating substituent on the 1,4-dioxolene bridge. We are currently addressing these issues.

Acknowledgment. The authors thank the EC−Joule Programme and the TMR Programme (CT96-0076) for financial assistance.

IC980293L